② IDŐJÁRÁS
Quarterly Journal of the Hungarian Meteorological Service
Vol. 114, No. 3, July – September 2010, pp. 217–227

Modeling of redline dayglow emission

Vir Singh[1*], **A. K. Upadhayaya**[2], and **M. V. Sunil Krishna**[1]

[1]*Department of Physics, Indian Institute of Technology Roorkee*
Roorkee – 247 667, India

[2]*Radio and Atmospheric Sciences Division, National Physical Laboratory,*
New Delhi – 110 012, India

[*]*Corresponding author; E-mail: virphfph@iitr.ernet.in*

(Manuscript received in final form August 8, 2008)

Abstract — The present paper deals with the morphological study of redline dayglow emission. The morphology is obtained from the profiles of redline dayglow emission using the updated Glow model. The Glow model is updated in terms of measured various collisional cross sections and reaction rate coefficients. The volume emission rate is obtained for some specific cases (18.3°S, 99.0°E, at 7:33 a.m. on February 1, 1993, 1.3°N, 139.0°E, at 11:30 a.m. on February 11, 1993, 35.2°S, 197.0°E, at 3:13 p.m. on April 2, 1993, and 52.9°S, 207.0°E, at 3:45 p.m. on April 9, 1993) using updated Glow model, and the results are compared with WINDII measurements. The modeled emission rate is found in good agreement with the WINDII observations at all altitudes except in the peak region where model underestimates the WINDII observations within 25%. The updated Glow model is further used to obtain the morphology of redline emission under equinox conditions (for the months of March and April, 1993) between 50°S and 50°N latitudes. It has been found that this emission shows an asymmetry between the Northern and Southern Hemispheres under equinox conditions. The asymmetry in the thermospheric region is likely due to the changing contributions with altitude of the various sources which are responsible for the production of $O(^1D)$ during daytime. The daytime intensity variation is found quite consistent with the WINDII measurements under equinox conditions.

Key-words: airglow, satellite observations, photochemistry, global emission intensity

1. Introduction

Redline dayglow emission is possibly the most extensively observed emission in the dayglow (*Noxon* and *Johanson*, 1972; *Narayan et al.*, 1989; *Sridharan et al.*, 1992; *Shepherd et al.*, 1993). It has now been well established that the redline dayglow emission shows a peak in upper thermospheric region (200 –230 km).

The well-known identified sources of redline dayglow emission are dissociative recombination, photoelectron impact on atomic oxygen, and photodissociation of O_2. However, the contribution of reaction of $N(^2D)$ with O_2 to the redline emission in airglow is still a matter of discussion (*Torr et al.*, 1981; *Link*, 1982; *Singh et al.*, 1996; *Link* and *Cogger*, 1988). Although, the altitude range of the production of $O(^1D)$ state extends from 100 to 300 km, the emission is mainly observed above 120 km, as below 120 km the $O(^1D)$ atoms are quenched by molecular nitrogen and molecular oxygen. A number of model calculations (*Hays et al.*, 1978; *Torr et al.*, 1981; *Bates*, 1990; *Singh et al.*, 1996; *Wittase et al.*, 1999) have been carried out to obtain volume emission rates (VER) of redline dayglow emission. These studies have only discussed the volume emission rate profile of 6300 Å in dayglow emission in the light of above mentioned production sources. From these studies one cannot have the idea about the global distribution of redline emission. The wind imaging interferometer (WINDII) has provided numerous data (*Shepherd et al.*, 1993) on redline dayglow emission along with the global distribution between 50°S and 50°N latitudes. WINDII measurements have thus provided an opportunity to study the morphology (volume emission rate as a function of altitude and latitude) of redline dayglow emission using theoretical models. The morphological study of 6300 Å would provide us valuable information about the relative distribution of this emission in both the hemispheres. The most reliable model that has been used to study the airglow emissions is the Glow model developed by *Solomon* (1992). After the development of this model, many input parameters, such as collisional cross-sections, reaction rate coefficients, and quantum yields, have been reexamined experimentally. Consequently the Glow model needs upgrade in light of the newly evaluated parameters.

In the present paper, the morphology of redline dayglow emission is studied in the altitude region of 120 to 300 km under equinox conditions at 10:00 a.m. in local time. The emission profiles are obtained using the Glow model of *Solomon* (1992). The Glow model is updated by using more recent cross-section data, reaction rate coefficients, and variation of solar fluxes. A comparison between the modeled morphology and the observed morphology from the WINDII measurements is made for a specific case for which WINDII data are available. The present morphology is used to discuss the relative variation of 6300 Å dayglow emission in both hemispheres.

2. Model

Mechanisms for the production of redline dayglow emission have been discussed by several workers (*Bates*, 1990; *Link* and *Swaminathan*, 1992; *Tyagi* and *Singh*, 2000), and the following reactions have been identified as the potential sources of redline emission in dayglow:

$$O(^3P) + e_{ph} \rightarrow O(^1D) + e_{ph}, \tag{1}$$

$$O_2^+ + e_{th} \xrightarrow{\eta_D k_2} O(^1S, ^1D, ^3P) + O(^3P), \tag{2}$$

$$N(^2D) + O_2 \xrightarrow{\eta_{2D} k_3} O(^1D) + NO \text{ (not confirmed)}, \tag{3}$$

$$O_2 + h\upsilon \rightarrow O(^1D) + O(^3P), \tag{4}$$

$$O(^1S) \xrightarrow{A_5} O(^1D) + h\upsilon \text{ (5577 Å)}. \tag{5}$$

In Eqs. (1) and (2), e_{ph} and e_{th} represent photoelectrons and thermal electrons, respectively. A_i and k_i represent the Einstein's coefficient and rate coefficients of the reactions. The production of $O(^1S)$ in Eq. (5) has been discussed by a number of workers (*Tyagi* and *Singh*, 1998; *Singh* and *Upadhayaya*, 2004) in detail. The $O(^1D)$ atoms are quenched by the following reactions:

$$O(^1D) + N_2 \xrightarrow{k_6} O(^3P) + N_2, \tag{6}$$

$$O(^1D) + O_2 \xrightarrow{k_7} O(^3P) + O_2, \tag{7}$$

$$O(^1D) \xrightarrow{A_8} O(^3P) + h\upsilon\text{(6300 Å)}. \tag{8}$$

The Glow model developed by *Solomon* (1992) is used in present calculations, and all the above sources of $O(^1D)$ have been included in the model. The neutral densities and neutral temperature have been used from MSISE-90 neutral atmosphere model (*Hedin*, 1991). The Glow model is updated by using more appropriate O excitation and ionization cross-sections, as given by *Kanik et al.* (1993). The total electron impact cross-section for O is taken as given by *Laher* and *Gilmore* (1990). The transport of photoelectrons and conjugate point effects as given by *Banks* and *Nagy* (1970) and *Nagy* and *Banks* (1970), respectively, have been included in the present calculations. The solar flux values are based on the full F74113 reference solar spectrum of *Hinteregger et al.* (1981), which is scaled using parameterization method based on F10.7 (daily 10.7 cm solar flux) and F10.7A (81 days average of the 10.7 cm solar flux). For ionizing EUV, the bin structure method of *Torr* and *Torr* (1985) is used in the present model. More details about the scaling techniques can be seen in *Upadhayaya* and *Singh* (2002) and *Tyagi* and *Singh* (2000). The total production rate of $O(^1D)$ at an altitude z is given by the following equation:

$$R_z[O(^1D)] = R_{EI}[O(^1D)] + R_{DR}[O(^1D)] + R_{N2D}[O(^1D)] + R_{DS}[O(^1D)] + R_{CAS}[O(^1D)], \quad (9)$$

where R_{EI}, R_{DR}, R_{N2D}, R_{DS}, and R_{CAS} are production rates of $O(^1D)$ due to individual sources for the reactions of Eqs. (1) – (5). Contributions for these individual sources have been discussed in more detail by *Tyagi* and *Singh* (2000). The volume emission rate of $O(^1D)$ at a particular altitude z is given by

$$V_z[O(^1D)] = Q_D R_z[O(^1D)], \quad (10)$$

Q_D is the quenching factor of $O(^1D)$ given by

$$Q_D = \frac{A_8}{A_8 + k_6[N_2] + k_7[O_2]}, \quad (11)$$

where A_8 is the Einstein coefficient for $O(^1D)$ state. The reactions and rate coefficients are given in *Table 1*.

Table 1. Reactions and rate coefficients

Reaction	**Rate coefficient ($cm^3\,s^{-1}$)**	**References**
$O(^3P) + e_{ph} \rightarrow O(^1D) + e_{ph}$	Impact cross-section	*Laher* and *Gilmore* (1990)
$O_2^+ + e_{th} \rightarrow O(^1D) + O(^3P)$	$k_2 = 1.6 \times 10^{-7}(300/T_e)^{0.5}$	*Walls* and *Dunn* (1974)
$N_2(^2D) + O_2 \rightarrow O(^1D) + NO$	$k_3 = 6.0 \times 10^{-12}$	*Lin* and *Kaufman* (1971)
$O(^1S) \rightarrow O(^1D) + h\upsilon$ (5577 Å)	$A_5 = 1.18\ s^{-1}$	*Nicolaides et al.* (1971)
$O(^1D) + N_2 \rightarrow O(^3P) + N_2$	$k_6 = 3 \times 10^{-11}$	*Hays et al.* (1978)
$O(^1D) + O_2 \rightarrow O(^3P) + O_2$	$k_7 = 2.9 \times 10^{-11}\exp(67.5/T_n)$	*Streit et al.* (1976)
$O(^1D) \rightarrow O(^3P) + h\upsilon$ (6300 Å)	$A_8 = 9.1 \times 10^{-3}\ s^{-1}$	*Nicolaides et al.* (1971)

3. Results and discussion

The 6300 Å dayglow volume emission rate profiles are obtained using the updated Glow model for several cases. However, to validate the model results, four cases are shown in *Fig. 1*. *Fig. 1a* shows the results for February 1, 1993 (35.2°S, 197.0°E, at 3:13 p.m., F10.7 = 125.1), *Fig. 1b* shows the results for February 11, 1993 (1.3°N, 139.0°E, at 11:30 a.m., F10.7 = 173.2), *Fig. 1c* shows the results for April 2, 1993 (18.3°S, 99.0°E, at 7:33 a.m., F10.7 = 120.8), and *Fig. 1d* shows the results for April 9, 1993 (52.9°S, 207.0°E, at 3:45 p.m., F10.7 = 135.5). WINDII data are available for these cases. It is quite clear from the values of F10.7 that these cases are for active days.

It is noticeable from *Fig. 1*, that the modeled results are in good agreement with the WINDII measurements except in the peak region, where the model underestimates the WINDII observations within 25%. Calculations have been performed for several other cases as well, and similar agreement is found with the WINDII observations. *Culot et al*. (2004) have also studied the redline emission using the TRANSCAR model and have compared their results with the WINDII observations. The TRANSCAR model also underestimates the WINDII observations, when the solar zenith angle (SZA) is less than 40°. The two cases for February 1, 1993 (*Fig. 1a*) and February 11, 1993 (*Fig. 1b*) have SZA less than 40°, where the model underestimates the WINDII observations within 25%. The other two cases for April 2, 1993 (*Fig. 1c*) and April 9, 1993 (*Fig. 1d*) have SZA greater than 40º, where the model is in very good agreement with the WINDII observations.

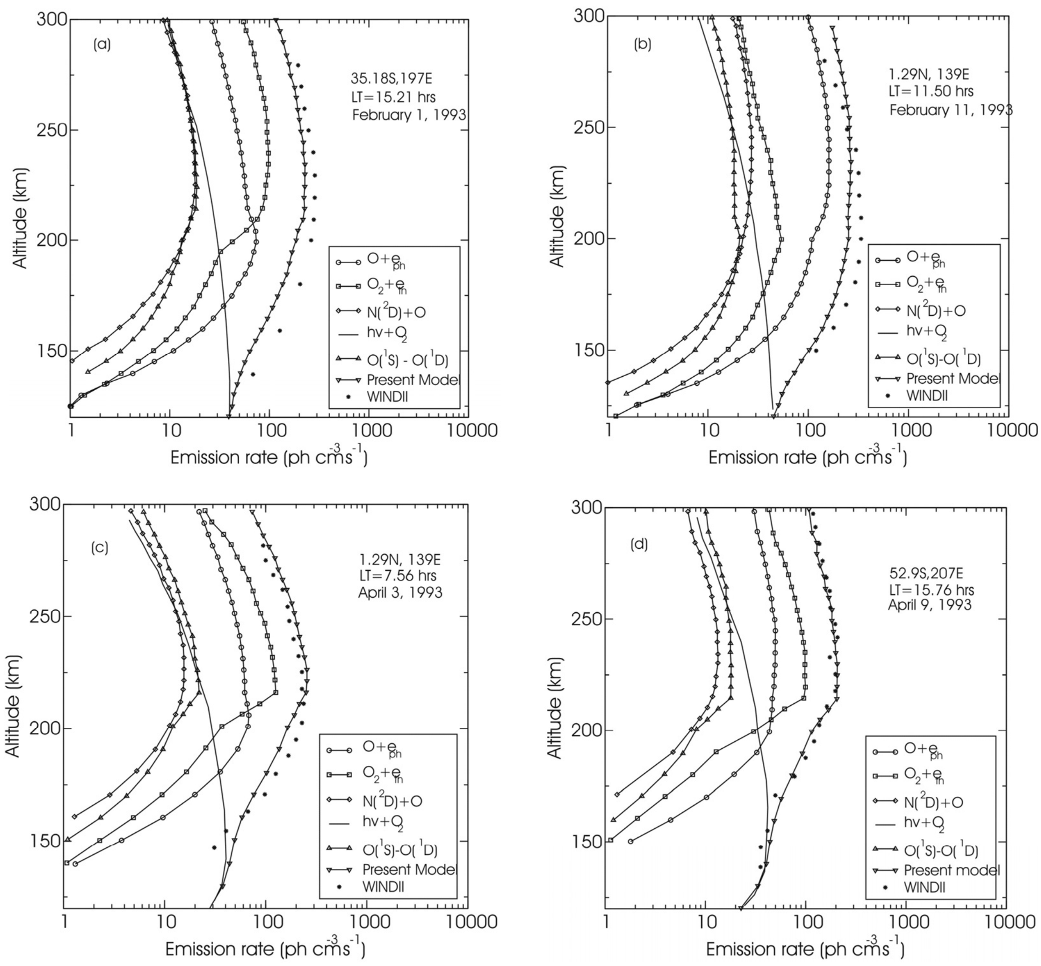

Fig. 1. Modeled and measured redline dayglow emission profiles for selected observing (WINDII) conditions with the various contributions of O(^{1}D) production processes.

The Glow model and the TRANSCAR model are thus quite consistent with each other. Volume emission rates of redline dayglow emission at various latitudes have been calculated along the track of satellite to obtain the morphology of this emission on February 11, 1993, for which WINDII data are available. On February 11, 1993 the WINDII started measurements of redline emission at 40°S, 2:07 UTC and ended the measurements at 50°N, 2:56 UTC. These observations are shown in *Fig. 2a*. It is quite evident from *Fig. 2a* that the WINDII observations show an asymmetry between the Northern and Southern Hemispheres for redline emission. The modeled morphology of redline emission for this case is shown in *Fig. 2b*. One can notice from *Fig. 2b* that the modeled morphology also shows the asymmetry between the Northern and Southern Hemispheres for the redline emission. It is relatively higher in the Northern Hemisphere than in the Southern Hemisphere between the 30° and 40° latitudes. *Fig. 2c* shows the percentage difference ((Glow model – WINDII / WINDII) × 100) between the modeled results and the WINDII observations for volume emission rate as a function of altitude and latitude for the above case. A close examination of *Fig. 2c* reveals that the modeled results are within 25% agreement with the WINDII observations in the altitude region of 180–220 km. At other altitudes the percentage difference between modeled and WINDII observation is very narrow (much smaller than 25 percent). Consequently, on the basis of the results shown in *Fig. 2c*, one may consider that the model is in good agreement with the WINDII observations.

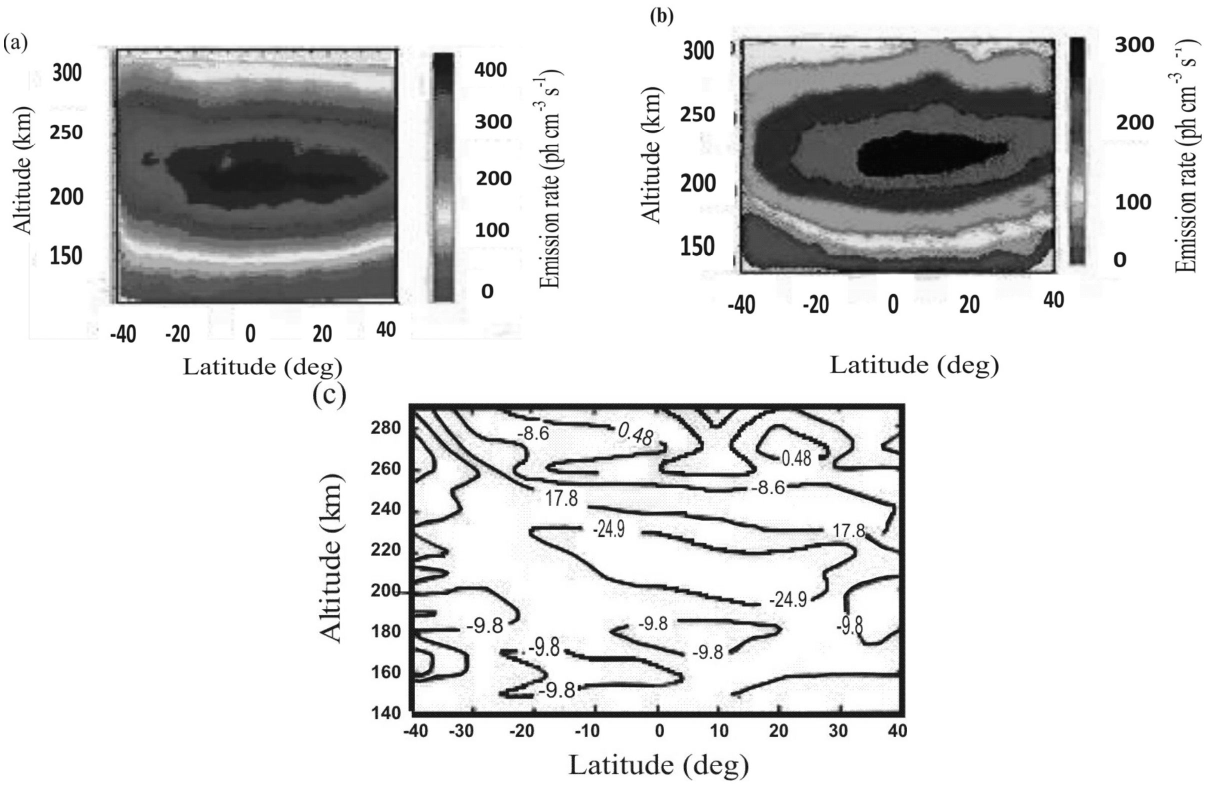

Fig. 2. (a) The altitude/latitude variation of volume emission rates as obtained from WINDII observations on February 11, 1993 (by courtesy of *G.G. Shepherd*). (b) The altitude/latitude variation of volume emission rates as obtained from model on February 11, 1993. (c) The percentage difference (((Glow model–WINDII)/WINDII) × 100) between the model calculations and WINDII observations on February 11, 1993.

The asymmetry of 6300 Å dayglow emission in both hemispheres can be best solved by studying the redline dayglow emission under equinox conditions (for the months of March and April). The reason to choose equinox case is that the sun is closer to the equator (approximate declination of 3°N). Note that this asymmetry in the illumination of the hemispheres due to the present location of the sun does not show any appreciable change (less than 3 percent) over the volume emission rates of redline dayglow emission obtained from the model in both hemispheres under the zero degree declination condition. Consequently, we may use this situation to identify the asymmetry of redline dayglow emission in both hemispheres. The 6300 Å dayglow volume emission rate profiles are obtained at various latitudes between 50°S and 50°N using the Glow model under equinox conditions. The volume emission rate profiles are obtained every fifth day starting from March 1, 1993 to April 30, 1993 at an interval of 5° latitude starting from 50°N, through the equator to 50°S at 10:00 a.m. using the Glow model. Averaging of volume emission rate is done for the above mentioned days for two months (March and April) at various altitudes for a fixed latitude. It would be worthwhile to mention here that the majority of the days during March and April 1993 were having the value of daily F10.7 solar flux greater than 110.

Fig. 3a shows the morphology of redline dayglow emission for 10:00 a.m. A close examination of the contours in *Fig. 3a* reveals that there is a clear asymmetry between the Northern and Southern Hemispheres in the thermospheric peak region (200–240 km) between the 20° and 50° latitudes. This asymmetry is clearly depicted in *Fig. 3b*, where the ratio of Northern to Southern Hemisphere volume emission rates is plotted as a function of altitude and latitudes. It is quite evident from *Fig. 3b* that the redline emission is about 15–20% higher in the Northern Hemisphere in comparison to the Southern Hemisphere between the 30° and 50° latitudes in the thermospheric peak region (200–240 km). The processes of dissociative recombination and photoelectron excitation of atomic oxygen are the dominating sources of this emission in this altitude region, and this, in, turn implies that the dissociative recombination and photoelectron excitation processes seem to be contributing more to redline emission in the Northern Hemisphere in comparison to the Southern Hemisphere. However, one can notice from *Fig. 1* that the contribution to redline emission due to dissociative recombination dominates over the photoelectron excitation contribution at midlatitudes. The TRANSCAR model (*Culot et al.*, 2004) also shows that the relative contribution due to the dissociative recombination process dominates over the photoelectron excitation contribution at midlatitudes. The production rate of $O(^1D)$ atoms due to the dissociative recombination process is proportional to the product of O_2^+ and thermal electron densities. Since, dissociative recombination process is the dominating source at midlatitudes, the asymmetry in redline emission may possibly be attributed due to higher densities of O_2^+ or thermal electrons in the

Northern Hemisphere in comparison to the Southern Hemisphere. However, this fact can only be ascertained if the simultaneous measurements of O_2^+ and thermal electron densities are available in both the hemispheres. It will be worthwhile to mention here, that the transport of photoelectrons is not symmetric about the geographic equator, because photoelectron fluxes are paired by conjugate points, which are not symmetric about geographic equator. Due to this fact, the production of redline emission due to photoelectron excitation process may vary from one hemisphere to another. This asymmetry may be a function of longitude. The results may vary from longitude to longitude. However, this longitudinal variation is not very prominent (the variation is within 5%) and has no strong bearing on the asymmetry of redline emission.

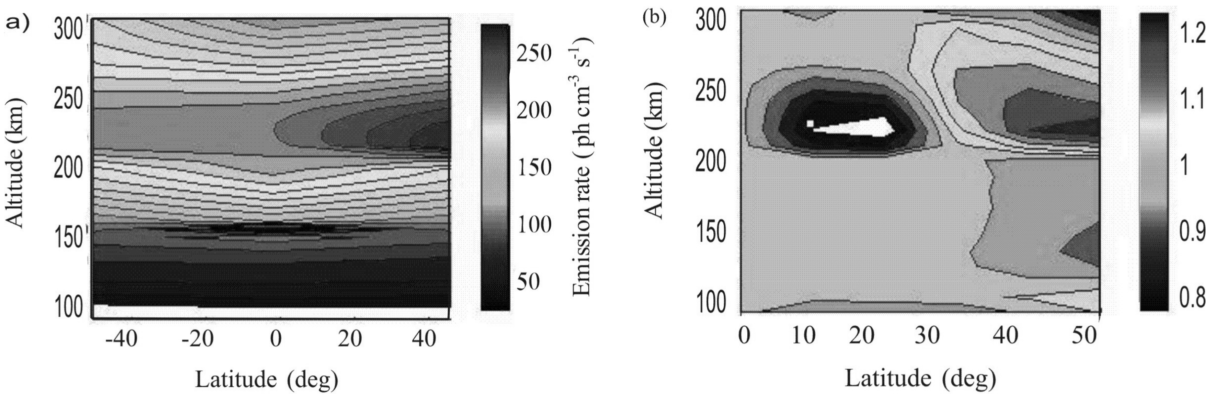

Fig. 3. (a) The altitude/latitude variation of two monthly (March–April 1993) averaged volume emission rates as obtained from model at 10:00 a.m. (b) The ratio of volume emission rate of the Northern to Southern Hemisphere as obtained from the model at 10:00 a.m.

There is no noticeable variation in the ratio of volume emission rates in the lower altitude region (120–180 km). In this altitude region, the photodissociation of O_2 is the dominating source of the production of $O(^1D)$ atoms. It indicates that the contribution to $O(^1D)$ by photodissociation process is more or less uniform in both hemispheres. In *Fig. 4*, the averaged latitudinal variation of intensity for redline dayglow emission is shown under equinox conditions at various local times. The intensities are obtained by integrating the volume emission rate over the vertical column of the altitude for every fifth day starting from March 1, 1993 to April 30, 1993 at an interval of 5° latitude starting from 50°N, through the equator, to 50°S at 8:00, 10:00, 12:00 a.m., 14:00 and 16:00 p.m. in local time. The averaging of intensities is done for the above mentioned days for two months (March and April) at various latitudes. The intensity reaches its maximum at noon, its magnitudes are quite similar at 10:00 a.m. and 2:00 p.m., and it obtaines relatively lower values at 8:00 a.m. and 4:00 p.m.

A variation in intensity from 1.6 KR to 2.1 KR depending on latitude and local time is seen for redline dayglow emissions. This is quite consistent with WINDII measurements as reported by *Zhang* and *Shepherd* (2004).

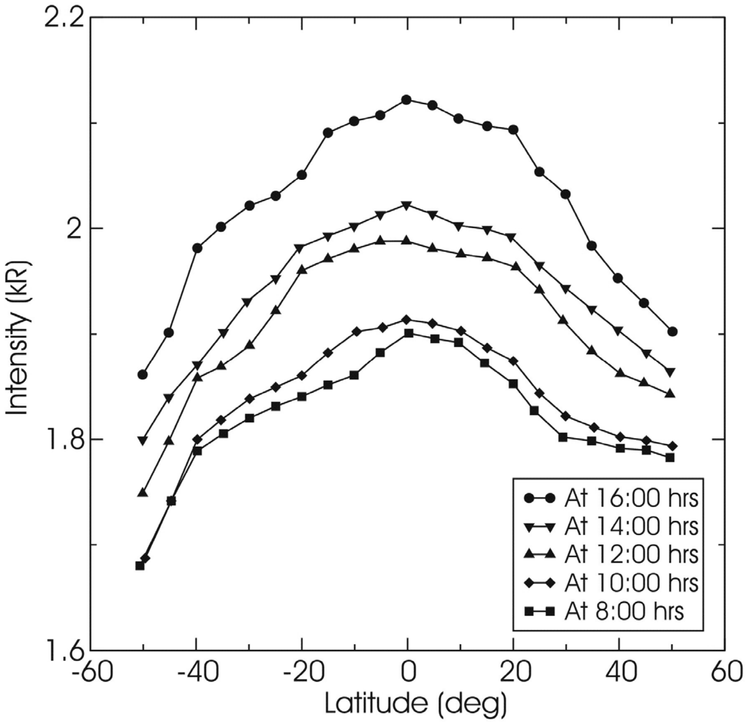

Fig. 4. Averaged latitudinal variation of intensity of 6300 Å dayglow emission under equinox conditions (March–April 1993) at various local times as obtained from the Glow model.

4. Conclusions

The morphology of redline dayglow emission has been studied using the updated Glow model between the 50°S and 50°N latitudes under equinox conditions (for the months of March and April 1993). It has been found that this emission shows an asymmetry between the Northern and Southern Hemispheres. It may be concluded that the asymmetry in the upper thermospheric region is likely due to the changing contributions of the dissociative recombination and photoelectron excitation processes with altitude and latitude. However, the dissociative recombination process seems to be more accountable for the asymmetry found in redline dayglow emission. The present study also indicates that the contribution to $O(^1D)$ by photodissociation process is more or less uniform in both hemispheres. A variation of 1.6 KR to 2.1 KR in intensity depending on latitude and local time is found for this emission, which is quite consistent with the WINDII observations.

Acknowledgement—The authors thank *Prof. G.G. Shepherd*, York University Canada for providing the WINDII data.

References

Banks, P.M. and *Nagy, A.F.,* 1970: Concering the influence of elastic scattering upon Photoelectron transport and escape. *J Geophys Res 75*, 1902-1910.

Bates, D.R., 1990: Oxygen green and redline emission and O_2^+dissociative recombination. *Planet Space Sci 38*, 889-902

Culot, F., Lathuillere, C. and *Lilensten, J.*, 2004: The OI 630.0 and 557.7 nm dayglow measured by WINDII and modeled by TRANSCAR. *Ann Geophys 22*, 1947-1960.

Hays, P.B., 1978: The OI(6300) airglow. *Rev Geophys Space Phys 16*, 225-232.

Hedin, A.E., 1991: Extension of the MSIS thermosphere model into the middle and lower atmosphere. *J Geophys Res 96*, 1159-1172.

Hinteregger, H., *Fukui, K.* and *Gilson, B.R.,* 1981: Observational references and model data on solar EUV, from measurements on AE-E. *Geophys Res Lett 8*, 1147-1150.

Kanik, K., Trajmar, S. and *Nickel, J.C.,* 1993: Total electron scattering and electronic state excitations cross sections for O_2, CO and CH_4. *J Geophys Res 98*, 7447-7460.

Laher, R.R. and *Gilmore, F.R.,* 1990: Updated excitation and ionization cross sections for electron impact on atomic oxygen. *J Phys Chem Ref Data 19*, 227-305.

Lin, C.-L. and *Kaufman, F*., 1971: Reactions of metastable nitrogen atoms. *J Chem Phys 55*, 3760-3771.

Link, R., 1982: Dayside magnetosphere cleft auroral processes. *Ph.D. Thesis*, York University, Canada.

Link, R. and *Cogger, L.L.*, 1988: A reexamination of the OI 6300 nightglow. *J Geophys Res 93*, 9883-9892.

Link, R.J. and *Swaminathan, P.K*., 1992: $N(^2D) + O_2$: A source of thermospheric 6300 Å emission. *Planet Space Sci 40*, 699-705.

Nagy, A.F. and *Banks, P.M.,* 1970: Photoelectron fluxes in the ionosphere. *J Geophys Res 75*, 6261-6270.

Narayanan, R. Desai, J.N. Modi, N.K. Raghavarao, R. and *Sridharan, R.,* 1989: Dayglow photometry: A new approach. *Appl Opt 28*, 2138-2142.

Nicolaides, C. Sinanoglu, O. and *Westhouse, P.,* 1971: Theory of atomic structure including electron correlation. IV. Method for forbidden transition probabilities with results for [OI], [OII], [OIII], [NI], [NII] and [CI]. *Phys Rev A4*, 1400-1410.

Noxon, J.F. and *Johanson, A.E*., 1972: Changes in thermospheric molecular oxygen abundance inferred from twilight 6300 Å airglow. *Planet Space Sci 20*, 2125-2151.

Shepherd, G.G. et al., 1993: WINDII, the wind imaging interferometer on the upper atmosphere research satellite. *J Geophys Res 98*, 10725-10750.

Singh, V. and *Upadhayaya, A.K*., 2004: Greenline dayglow emission under equinox conditions. *J Geophys Res 109*, A01308.

Singh, V., McDade, I.C., Shepherd, G.G., Solheim, B.H. and *Ward, W.E.,* 1996: The $O(^1D)$ dayglow emissions as observed by the WIND imaging interferometer on the UARS. *Adv Space Res 17*, 11-14.

Solomon, S., 1992: *Glow Model Version 0.95*. LASP, University of Colorado, Boulder, USA.

Sridharan, R., Haider, S.A., Gurubaran, S., Sekar, R. and *Narayanan, R.,* 1992: OI 630.0nm dayglow in the region of equatorial ionization anomaly: Temporal variability and its causative mechanism. *J Geophys Res 97*, 13715-13721.

Streit, G.E., Carleton, J.H., Schmeltekopf, A.L., Davidson, J.A. and *Schiff, H.I.,* 1976: Temperature dependence of $O(^1D)$ rate constants for reactions with O_2, N_2, CO_2,O_3 and H_2O. *J Chem Phys 65*, 4761-4764.

Torr, M.R. and *Torr, D.G.,* 1985: Ionization frequencies for solar cycle 21: revised. *J Geophys Res 90*, 6675-6678.

Torr, D.G., Richards, P.G., Torr, M.R. and *Abreu, V.J.,* 1981: Further quantification of the sources and sinks of thermosphere $O(^1D)$ atoms. *Planet Space Sci 29*, 595-600.

Tyagi, S. and *Singh, V*., 1998: The morphology of oxygen greenline dayglow emission. *Ann Geophys 16*, 1599-1606.

Tyagi, S. and *Singh, V.*, 2000: Re-examination of reaction of $N(^2D)$ with O_2 as a source of $O(^1D)$ in dayglow emission. *Indian J Radio Space Phys 29*, 291-295.
Upadhayaya, A.K. and *Singh, V.*, 2002: Effects of temperature dependence of reaction $N_2(A^3\Sigma_u^+) + O$ on greenline dayglow emission. *Ann Geophys 20*, 2039-2045.
Walls, F.L. and *Dunn, G.H.*, 1974: Measurement of total cross sections for electron recombination with NO^+ and O_2^+ using ion storage techniques. *J Geophys Res 79*, 1911-1915.
Wittase, O., Lilensten, J., Lathuilliere, C. and *Blelly, P.L.,* 1999: Modeling the OI 630.0 and 557.7 nm thermospheric dayglow during EISCAT-WINDII coordinated measurements. *J Geophys Res 104*, 24.639-24.656.
Zhang, S.P. and *Shepherd, G.G.*, 2004: Solar influence on $O(^1D)$ dayglow emission rate: Global -scale measurement by WINDII on UARS. *Geophys Res Lett 31*, L07804.